Green Chemistry

RSC Publishing

PAPER

View Article Online
View Journal | View Issue

Cite this: *Green Chem.*, 2013, **15**, 1238

Efficient three-component coupling catalysed by mesoporous copper–aluminum based nanocomposites†

Jana Dulle,[a] K. Thirunavukkarasu,[b] Marjo C. Mittelmeijer-Hazeleger,[c] Daria V. Andreeva,*[a] N. Raveendran Shiju*[c] and Gadi Rothenberg*[c]

Received 16th August 2012,
Accepted 30th January 2013

DOI: 10.1039/c3gc36607c

www.rsc.org/greenchem

Traditional synthesis methods for propargylamines have several drawbacks. A recently developed alternative route is the so-called "A^3 coupling" in which an alkyne, an aldehyde, and an amine are coupled together. Typically, these reactions are catalysed by homogeneous gold salts, organogold complexes or silver salts. But these homogeneous catalysts are expensive and their separation is difficult. Here we report the discovery that solid Cu/Al/oxide mesoporous "sponges" are excellent A^3 coupling catalysts. These materials are robust, inexpensive, and easy to make. They give good to excellent yields (87–97%) for a wide range of substrates. Being heterogeneous, these catalysts are also easy to handle and separate from the reaction mixture, and can be recycled with no loss of activity.

One of the biggest challenges in organic chemistry is mimicking the complexity of biosynthesis *in vitro*. Nature excels at matching multiple simple substrates in one-pot reactions that give complex molecules with high yields.[1–4] We chemists can also do this, but typically using a host of stoichiometric reagents and protecting groups, and often generating much waste in the process.

The synthesis of propargylic amines is a good example. These amines are key intermediates for making drugs and agrochemicals.[5–8] They are traditionally synthesized by nucleophilic attack of lithium acetylides or Grignard reagents on imines or their derivatives.[9,10] However, such reagents must be used stoichiometrically, causing large amounts of waste. They are also moisture-sensitive, and require strictly controlled reaction conditions.

An elegant alternative route is the so-called "A^3 coupling" (eqn (1)). This catalytic reaction between an alkyne, an aldehyde, and an amine (hence the three A's) gives water as the only by-product.[7,11] The reaction is run in a liquid phase, using homogeneous catalysts such as gold salts,[12] organogold complexes,[13] silver salts,[14–17] and Hg_2Cl_2.[18] Among these, the gold salts show the highest activity. The problem is that rapid reduction of cationic gold species to inactive metallic atoms is unavoidable when gold salts activate alkynes/alkenes.[19–21] Moreover, using homogeneous catalysts brings inherent complications in catalyst separation and reuse. The ideal solution, therefore, would be replacing the homogeneous gold salt with an effective, yet inexpensive, heterogeneous catalyst.[22–35] Many of the heterogeneous catalysts are supported/immobilized gold nanoparticles.[36] Zhang *et al.* reported that supported gold is active for the A^3 coupling reaction.[21] Also, gold nanoparticles embedded in a mesoporous carbon nitride support was shown to be an efficient heterogeneous catalyst for the synthesis of propargylamines, although its catalytic efficiency has been demonstrated for very few substrates.[37] Another active catalyst is gold nanoparticles supported on nanocrystalline MgO.[38] The silver salt of 12-tungstophosphoric acid ($Ag_3PW_{12}O_{40}$) was also used to catalyse the A^3-coupling.[39] Gold and copper thin films were used as catalysts in microwave-assisted continuous-flow organic synthesis (MACOS) of propargylamines[40]. Liu *et al.* reported gold functionalized IRMOF-3 catalysts for the one-pot synthesis of propargylamines.[41] In another report, gold nanoparticles impregnated on alumina was used as a catalyst for propargylamine synthesis in a flow reactor.[34] Considering the costs, it would be better to have an active catalyst containing no precious metals. A recent review by Peshkov *et al.* summarised the homogeneous and heterogeneous catalysts utilized in A^3-coupling.[42]

We now report the discovery that copper/aluminum (Cu/Al) based mesoporous nanocomposites are excellent A^3 coupling catalysts. These materials are robust, inexpensive, and easy to

[a]*Physical Chemistry II, University of Bayreuth, Universitätsstr. 30, 95447 Bayreuth, Germany. E-mail: daria.andreeva@uni-bayreuth.de; Fax: +49 (0)921 55 2059; Tel: +49 (0)921 55 2750*

[b]*National Centre for Catalysis Research, Indian Institute of Technology-Madras, Chennai-600 036, India*

[c]*Van't Hoff Institute for Molecular Sciences, University of Amsterdam, Science Park 904, 1098 XH Amsterdam, The Netherlands. E-mail: n.r.shiju@uva.nl, g.rothenberg@uva.nl; Fax: +31 (0)20525 5604; Tel: +31 (0)20525 6515 http://www.hims.uva.nl.hcsc*

†Electronic supplementary information (ESI) available: Pore-size distribution of catalyst and ^{1}H NMR spectral data. See DOI: 10.1039/c3gc36607c

make. They are highly active in the coupling reaction of aldehydes, amines, and alkynes, giving propargylamines selectively with water as the only by-product.

The catalysts are essentially RANEY®-type materials, though our method for making them differs from the RANEY® process.[43] We create first a Cu/Al alloy, and then use intense sonication for fragmenting and partially oxidising the particles (see the Experimental section for detailed procedures).[44–47]

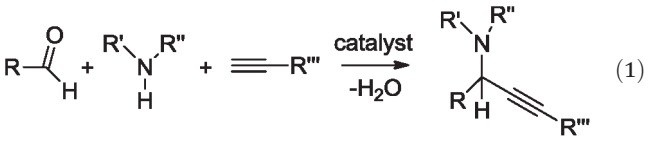

(1)

This simple and waste-free route is based on our recent finding that ultrasound can cause re-structuring of metal alloys due to cavitation induced microphase separation (Fig. 1). During sonication the metal alloy particles undergo the sonomechanical and sonochemical effects stimulated by cavitation. These effects lead to fragmentation, surface reactions, and formation of pores. The metals in the alloy have different chemical (standard electrode potentials) and physical (melting points and hardness of the oxide layer) properties. Thus, the rates of the above processes are different for the alloy components. In the case of Cu/Al, this gives a mesoporous aluminum-based framework, with homogeneously distributed oxidized copper particles. This morphology of the Cu/Al particles has several attractive features for heterogeneous catalysis: increased surface area, mesopores, and unique textural stability.

Benzaldehyde, piperidine, and phenylacetylene were used as model substrates to study the catalytic activity of the Cu/Al catalyst in A^3 coupling. Our catalyst gave high benzaldehyde conversion (~99%), as well as a high yield of the coupling product (see Table 1). Control experiments confirmed that no conversion was found in the absence of catalyst under otherwise identical conditions. Compared with commercial Cu_2O (Cu^+ is predominant in our catalyst; see below the XPS characterization) the sample was not as active and selective to A^3 coupling, under the same conditions. Homocoupling of the alkyne was also observed in this case and selectivity to the A^3 coupled product was only 60%. Indeed, homogeneous copper salts were also reported to be active as catalysts, but again these gave only moderate conversions and selectivities.[48–51] Moreover, difficulties in recovering the catalyst from the reaction mixture limit their use.

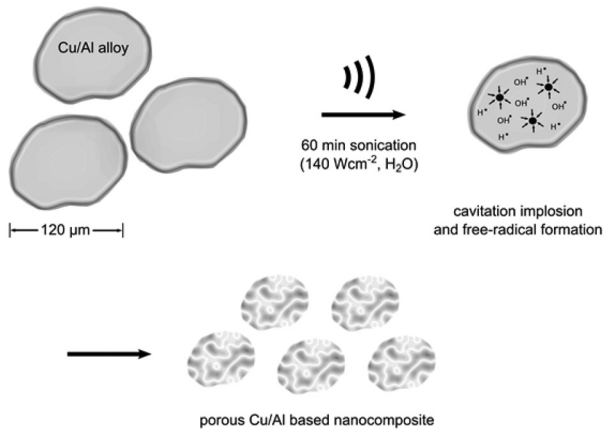

Fig. 1 Sonochemical formation of mesoporous Cu/Al based particles. Intensive sonication of the initial alloy particles leads to fragmentation, porosity, and surface oxidation.

Table 1 A^3 coupling catalyzed by Cu/Al

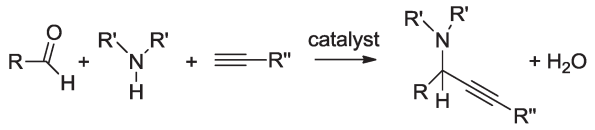

Entry	R[a] (aldehyde)	R′$_2$NH (amine)	R″ (alkyne)	Yield (GC/isolated)[b]
1	Ph	Piperidine	Ph	99/94
2	4-$CH_3C_6H_4$	Piperidine	Ph	93/87
3	Cyclohexyl	Piperidine	Ph	97/90
4	3-ClC_6H_4	Piperidine	Ph	96
5	3-OHC_6H_4	Piperidine	Ph	92
6	3-$NO_2C_6H_4$	Piperidine	Ph	88
7	Ph	Morpholine	Ph	94/88
8	Ph	Pyrrolidine	Ph	90
9	Ph	Piperidine	Hexyl	92
10	Ph	Piperidine	4-$CH_3C_6H_4$	95
11	Ph	Piperidine	4-$CH_3OC_6H_4$	90
12	4-$OCH_3C_6H_4$	Piperidine	Ph	94
13	Ph	Piperidine	Ph	45[c]
14	Ph	Piperidine	Ph	92[d]
15	Ph	Piperidine	Ph	81[e]

[a] Reaction conditions: aldehyde (1.0 mmol), amine (1.2 mmol), and alkyne (1.3 mmol), Cu/Al (0.12 mmol Cu), toluene (1.7 ml), 100 °C, 22 h; [b] mol% of A^3 coupling product yield based on aldehyde starting material (entries 1–12, complete conversion monitored by GC); [c] Cu_2O catalyst, 75% conv.; [d] Cu/Al, 90 °C, 22 h (GC conv. 92%); [e] Cu/Al, 70 °C, 22 h (GC conv. 82%).

Kantam *et al.* showed that CuO nanoparticles gave a good yield for A^3 coupling, while commercially available bulk Cu_2O and bulk CuO gave poor yields.[35] The yield was 82% using benzaldehyde, piperidine and phenylacetylene using toluene as the solvent. The yield varied from 8% to 84% when the substrates were changed. Recently, Albaladejo *et al.* reported that Cu_2O on titania is a good catalyst for A^3 coupling.[52] The catalyst was prepared by supporting copper nanoparticles, made by the addition of $CuCl_2$ to a suspension of lithium and 4,4′-di-*tert*-butylbiphenyl in THF, on TiO_2. They obtained 32% yield (using toluene as the solvent) and 98% yield (using neat substrate) starting from benzaldehyde, piperidine and phenylacetylene. For other substrates, the yield of the A^3 coupled products varied, from 52% to 98%. Notwithstanding these results, our Cu/Al catalyst gives complete conversion to the A^3

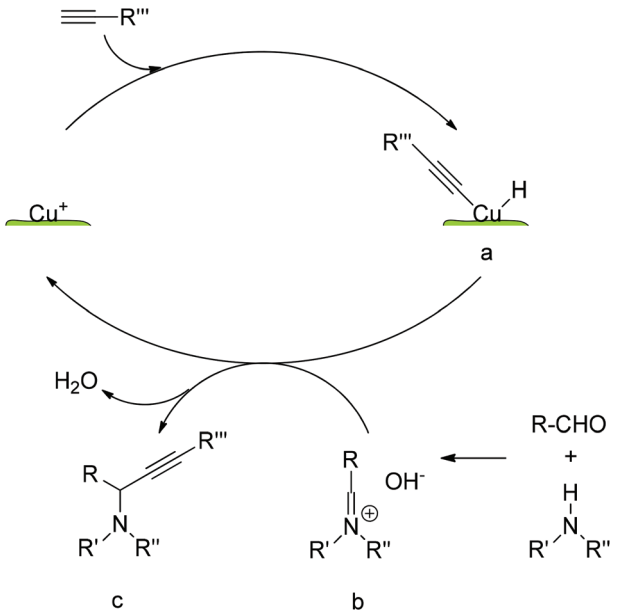

Scheme 1 Tentative mechanism of the A^3 coupling. The Cu(I) species activates the C–H bond of the alkyne to give a copper acetylide intermediate (a), which reacts with the immonium ion (b) generated *in situ* from the aldehyde and secondary amine to give the corresponding propargylamine (c).

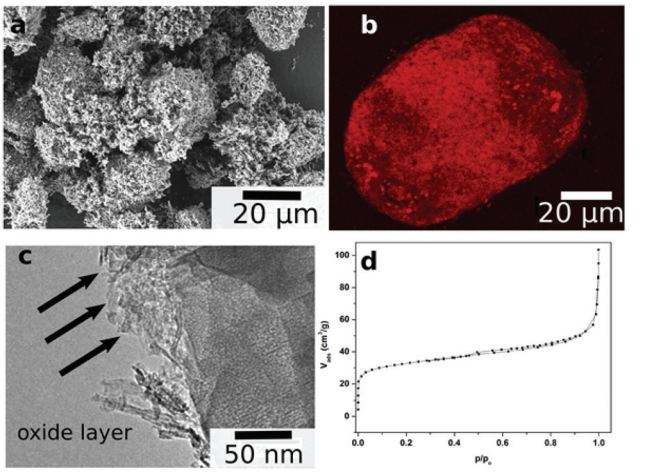

Fig. 2 Scanning electron micrograph (a), 3D confocal microscopy reconstruction of the particle loaded with rhodamine B (picture taken in fluorescent mode) showing the porosity throughout the catalyst particle (b), transmission electron micrograph (c), and nitrogen adsorption isotherm (d) of the Cu/Al catalyst, showing the morphology and porous structure.

product in toluene, as well as high activity for different substrates as well, with 88%–99% yield. This matches and in some cases outperforms gold catalysts published elsewhere. Thus, Wei *et al.* reported that AuCl, AuI, $AuBr_3$, and $AuCl_3$ showed good activities for A^3 coupling.[12] The yield of propargylamines ranged from 53% to 99%, depending on the substrates. Zhang *et al.* showed that Au/CeO_2 catalyses A^3 coupling and the yield varies from 25%–99%, again depending on the substrates.[21] Another report shows that gold nanoparticles embedded in a mesoporous carbon nitride catalyses the A^3 coupling, yielding 51% after 12 h and 62% after 24 h.[37]

We believe that the reaction mechanism (Scheme 1) involves the formation of copper acetylide, as was proposed for A^3 coupling with cationic gold under homogeneous conditions.[12,28] Recently, Albaladejo *et al.* demonstrated that A^3 coupling using heterogeneous Cu/TiO_2 also involves copper acetylide formation.[52] The same mechanism can be invoked in our system. Thus, the C–H bond of the alkyne is activated by a Cu(I) species to give a copper acetylide intermediate (a), which reacts with the immonium ion (b) generated *in situ* from the aldehyde and secondary amine to give the corresponding propargylamine (c) and regenerate the catalytically active site.

Understanding the structure and the morphology of the catalyst surface is the key to understanding its activity. Therefore, we carried out a series of characterisation experiments. Electron microscopy (Fig. 2a and 2c) showed that the initial particles of ~120 μm are broken into ~40 μm pieces after 60 min of sonication. The SEM and TEM images show a porous interfacial layer. Combining this with N_2 adsorption studies (Fig. 2d) we confirm the formation of a porous outer surface and modification of the inner structure, increasing the specific surface area to 34 $m^2\ g^{-1}$. The BET isotherm is type II.[53] We see that the monolayer coverage is completed and multilayer N_2 adsorption starts at a relative pressure of *ca.* 0.03. This shows that the material has both micropores and mesopores. The meso and micropore areas were 11.2 $m^2\ g^{-1}$ and 22.8 $m^2\ g^{-1}$ and the meso and micropore volumes were 0.03 $cm^3\ g^{-1}$ and 0.01 $cm^3\ g^{-1}$ (pore size distribution is given in ESI†).

We also examined the inner structure of the material by monitoring the spatial distribution of a fluorescent dye inside the particles. Fig. 2b shows a 3D reconstruction of confocal scanning fluorescence microscopy (CSFM) images of a catalyst particle loaded with rhodamine B. Here, too, we can see the porous inner structure.

The powder X-ray diffraction (PXRD) pattern of the initial alloy showed intense peaks for Al and $CuAl_2$ (Fig. 3). After sonication, the PXRD reveals the peaks corresponding to highly ordered $Al(OH)_3$ (bayerite) crystallites and CuO, thus, partial oxidation of the alloy. The different Cu/Al mixed phases also can be distinguished in the PXRD pattern of the modified particle, indicating an increased interaction between the two metals.

Using XPS, we observed mixed oxidation states for Cu on the catalyst surface (Fig. 4 and Table 2). The majority (72%) of the copper on the surface was Cu^+, with a binding energy (BE) of 932.5 eV. The rest is Cu^{2+} (BE = 933.7 eV). Indeed, low intensity satellite features (exclusively due to Cu^{2+}) support the minor contribution from the latter. However, because Cu^0 and Cu^+ states have the same BE, we also recorded the X-ray-excited Auger electron spectroscopy (XAES) for the Cu LMM region. The Cu LMM peak can be resolved into two distinct peaks (see Fig. 4, inset) at 914.2 eV (kinetic energy, KE) and 917.7 eV. These correspond to Cu^+ and Cu^{2+}, respectively. The presence of Cu^{2+} was further confirmed by the satellite peaks (denoted by arrows in Fig. 4). The absence of an ~918.5 eV KE

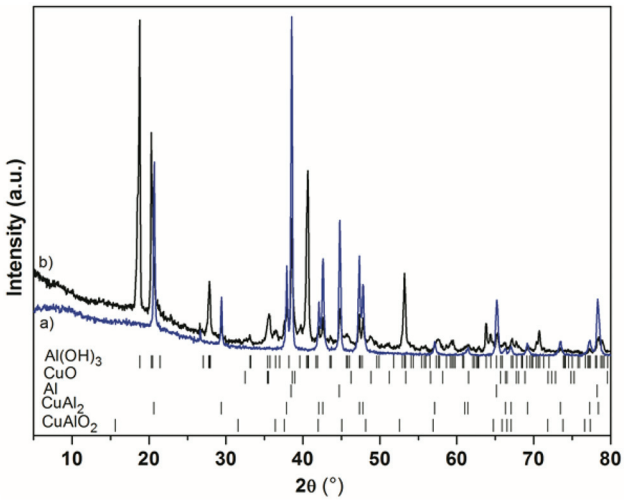

Fig. 3 PXRD patterns of the initial particles (a) and particles sonicated for 60 min (b).

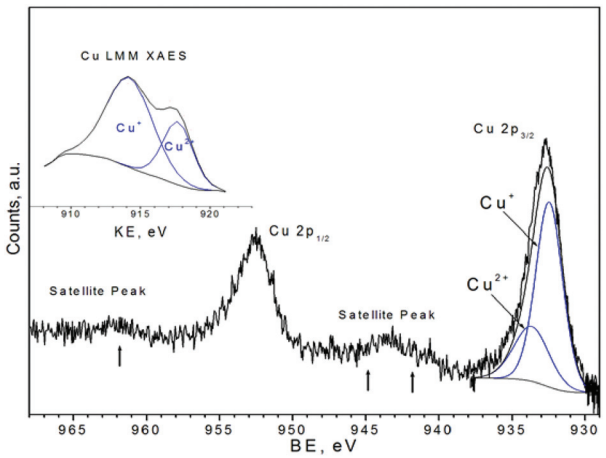

Fig. 4 Cu 2p XP spectrum of Cu/Al; the inset shows the Cu LMM XAE spectrum (tabulated data are provided in Table 2).

Table 2 XPS data of the Cu/Al sample

Core level	Binding energy (eV)	FWHM (eV)
Al 2p	73.7	1.87
O 1s	531.3	2.55
Cu 2p (Cu^{+})	932.5 (914.2[a])	2.18
Cu 2p (Cu^{2+})	933.7 (917.7[a])	2.83

[a] Kinetic energy values of the Cu LMM XAE spectra.

feature in the spectra shows that there is no Cu^0 in the sample.[54,55] Moreover, the negative shift in the BE of the Al 2p core level (73.7 eV) compared with the Al 2p of the Al_2O_3 support alone (~74 eV) indicates a metal-to-support electron transfer process. The interaction between the Cu and the support and consequent modification of the electronic environment may be responsible for the high selectivity of the catalyst, compared to the bulk Cu_2O. Since the XRD did not show peaks corresponding to Cu_2O, it is either amorphous or highly dispersed on the Al surface.

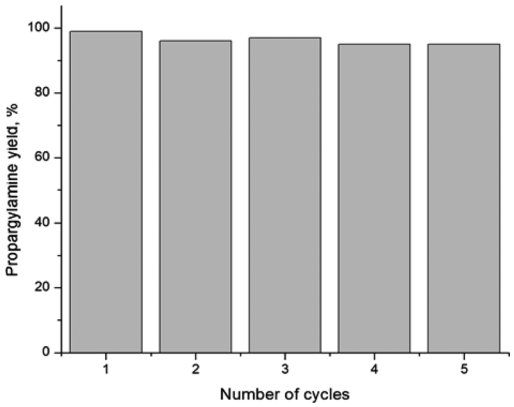

Fig. 5 Catalyst recycling studies in the coupling of phenyl acetylene, benzaldehyde and piperidine. Reaction conditions: aldehyde (1.0 mmol), amine (1.2 mmol), and alkyne (1.3 mmol), Cu/Al (0.12 mmol Cu), toluene (1.7 ml), 100 °C, 22 h. After each cycle, the catalyst was filtered, washed with acetone and water and dried at 403 K.

To test catalyst reusability, we ran five consecutive reaction cycles. After each cycle, the catalyst was filtered, washed with acetone and water and dried at 403 K. The results were similar to the original reaction and no significant deactivation was observed, confirming the reusability of our catalyst (Fig. 5).

Conclusions

We showed here that the A^3 coupling reaction can run in the presence of a solid catalyst that contains only copper, aluminum, and oxygen. This catalyst is stable. It is readily recovered after the reaction and can be recycled several times without deactivation. The process is simple and general, giving propargylamines in good to excellent yields for a variety of substrates. Finally, the fact that our catalyst contains neither noble nor heavy or toxic metals opens true opportunities for practical application.

Experimental section

Materials and instrumentation

Aluminium shot (irregular, <15 mm, 99.9%; metal basis) and copper beads (2–8 mm, 99.9995%; trace metals basis) were purchased from Alfa Aesar and Sigma Aldrich, respectively, and used as received. Water was purified using a three-stage Millipore Milli-Q Plus 185 purification system (final resistivity >18.2 MΩ cm).

Transmission and scanning electron microscopes (TEM, Zeiss 922 EFTEM operating at 200 kV and Zeiss 1530 FE-SEM respectively) in combination with an ultra-microtome (Ultracut E Reichert Jung, thickness 50 nm) were applied to characterise the optical response, structure, and size of the Cu/Al powder.

Powder X-ray diffraction data were collected on a Stoe STADI P X-ray diffractometer using Cu $K\alpha_1$ radiation at room temperature. The N_2 adsorption–desorption isotherms were measured at 77 K on a vacuum gas sorption apparatus Surfer (Thermo Scientific), after evacuation at 300 °C for 24 h. The surface area was calculated by the BET method. X-ray photoelectron spectroscopy (XPS) measurements were carried out using a multiprobe system (Omicron Nanotechnology, Germany) equipped with a dual Mg/Al X-ray source and a hemispherical analyzer operating in constant analyzer energy (CAE) mode. The spectra were obtained with a pass energy of 50 eV for the survey scan and 20 eV for individual scans. A Mg Kα X-ray source was operated at 300 W and 15 kV. The base pressure in the analyzing chamber was maintained at 1×10^{-10} mbar. The data were processed with the Casa XPS program (Casa Software Ltd, UK), and calibrated with reference to the adventitious carbon peak (284.9 eV) in the sample. Peak areas were determined by integration employing a Shirley-type background. Peaks were considered to be a 70 : 30 mix of Gaussian and Lorentzian functions. The relative sensitivity factors (RSF) provided by the manufacturer were used for quantifying elements.

Procedure for catalyst preparation

Aluminium and copper were first alloyed using an AM arc melter (Edmund Bühler GmbH, Germany) with a melt stream of 300 A. The reactor was first evacuated to 10^{-5} mbar and then pressurised to 500 mbar argon. For homogenization, the sample was overturned three times and fused each time. The bulk material was cut into pieces and ground using a rotary mill (Pulverisette 14, Fritsch GmbH, Germany) with a sieve ring of 0.12 mm. The resulting powder (typically 30 g alloy, 25.0 wt% Cu) was then sieved by a 150 μm sieve.

Five grams of this Cu/Al alloy were then dispersed in 50 ml purified water and sonicated for 60 min with an ultrasound tip (VIP1000hd, Hielscher Ultrasonics GmbH, Germany). The device was operated at 20 kHz with a maximum output power of 1000 W by an ultrasonic horn BS2d22 (head area of 3.8 cm^2). It was equipped with a booster B2–1.8 for 60 min. The maximum intensity was calculated to be 140 W cm^{-2} at a mechanical amplitude of 106 μm. To avoid the temperature increase during sonication the experiment was performed in a thermostatic cell. The resulting powder was then dried at 120 °C for 5 h.

General procedure for Cu/Al-catalysed A^3 coupling

The amine (1.2 mmol), aldehyde (1.0 mmol), alkyne (1.3 mmol), Cu/Al (0.12 mmol based on Cu) and toluene (1.7 ml) were added to a 50 ml round-bottom flask equipped with a magnetic stirring bar and connected to a water-cooled condenser. The mixture was degassed and backfilled with nitrogen, and then stirred for 22 h at 100 °C (oil bath). After the reaction, the mixture was cooled to ambient temperature and the catalyst was filtered. The residue was washed with an additional 5 ml toluene, which was then combined with the filtrate. The samples were analyzed by gas chromatography (VB-1 column, FID), and/or purified by column chromatography (silica gel; hexane : EtOAc 4 : 1) and analysed using ^{1}H NMR. Product identity and purity was confirmed by ^{1}H NMR spectroscopy and mass spectrometry.

Example: N-(1,3-Diphenyl-2-propynyl)piperidine (Table 1, entry 1): Benzaldehyde (1.0 mmol, 106.1 mg), piperidine (1.2 mmol, 102.2 mg), phenylacetylene (1.3 mmol, 132.8 mg), Cu/Al catalyst (0.12 mmol based on Cu, 30 mg), and toluene (1.7 ml) were reacted and analysed as above (258 mg, 94% yield). ^{1}H NMR δ = 7.00–7.65 (m, 10H), 4.80 (s, 1H), 2.40–2.60 (m, 4H), 1.56–1.69 (m, 4H), 1.30–1.50 (m, 2H); MS *m*/*z* (%) 275 (M^+, 20), 274 (10), 191 (100), 198 (79), 192 (24), 189 (24), 115 (14), 165 (10), 232 (8).

Acknowledgements

We thank Dr C.S. Gopinath (National Chemical Laboratory, Pune) for his suggestions on XPS measurements and B. Putz (University of Bayreuth) for the PXRD measurements. J. D. and D. A. thank SFB 840 for financial support.

Notes and references

1 K. C. Nicolaou, D. J. Edmonds and P. G. Bulger, *Angew. Chem., Int. Ed.*, 2006, **45**, 7134–7186.
2 B. M. Trost, *Science*, 1991, **254**, 1471–1477.
3 M. K. Singh and M. K. Lakshman, *J. Org. Chem.*, 2009, **74**, 3079–3084.
4 J. W. Lee, T. Y. Kim, Y.-S. Jang, S. Choi and S. Y. Lee, *Trends Biotechnol.*, 2011, **29**, 370–378.
5 A. A. Boulton, B. A. Davis, D. A. Durden, L. E. Dyck, A. V. Juorio, X.-M. Li, I. A. Paterson and P. H. Yu, *Drug Dev. Res.*, 1997, **42**, 150–156.
6 M. Miura, M. Enna, K. Okuro and M. Nomura, *J. Org. Chem.*, 1995, **60**, 4999–5004.
7 T. Naota, H. Takaya and S.-I. Murahashi, *Chem. Rev.*, 1998, **98**, 2599–2660.
8 L. Zani and C. Bolm, *Chem. Commun.*, 2006, 4263–4275.
9 M. E. Jung and A. Huang, *Org. Lett.*, 2000, **2**, 2659–2661.
10 T. Murai, Y. Mutoh, Y. Ohta and M. Murakami, *J. Am. Chem. Soc.*, 2004, **126**, 5968–5969.
11 G. Dyker, *Angew. Chem., Int. Ed.*, 1999, **111**, 1808–1822.
12 C. Wei and C.-J. Li, *J. Am. Chem. Soc.*, 2003, **125**, 9584–9585.
13 V. K.-Y. Lo, Y. Liu, M.-K. Wong and C.-M. Che, *Org. Lett.*, 2006, **8**, 1529–1532.
14 C. Wei, Z. Li and C.-J. Li, *Org. Lett.*, 2003, **5**, 4473–4475.
15 Z. Li, C. Wei, L. Chen, R. S. Varma and C.-J. Li, *Tetrahedron Lett.*, 2004, **45**, 2443–2446.
16 K. Mohan Reddy, N. Seshu Babu, I. Suryanarayana, P. S. Sai Prasad and N. Lingaiah, *Tetrahedron Lett.*, 2006, **47**, 7563–7566.
17 Y. Zhang, A. M. Santos, E. Herdtweck, J. Mink and F. E. Kuhn, *New J. Chem.*, 2005, **29**, 366–370.
18 L. Pin-Hua and W. Lei, *Chin. J. Chem.*, 2005, **23**, 1076–1080.

19 A. Hoffmann-Roder and N. Krause, *Org. Biomol. Chem.*, 2005, **3**, 387–391.
20 X. Zhang and A. Corma, *Chem. Commun.*, 2007, 3080–3082.
21 X. Zhang and A. Corma, *Angew. Chem., Int. Ed.*, 2008, **47**, 4358–4361.
22 M. L. Kantam, B. V. Prakash, C. R. V. Reddy and B. Sreedhar, *Synlett*, 2005, 2329–2332.
23 W. Yan, R. Wang, Z. Xu, J. Xu, L. Lin, Z. Shen and Y. Zhou, *J. Mol. Catal. A: Chem.*, 2006, **255**, 81–85.
24 B. M. Choudary, C. Sridhar, M. L. Kantam and B. Sreedhar, *Tetrahedron Lett.*, 2004, **45**, 7319–7321.
25 A. Fodor, A. Kiss, N. Debreczeni, Z. Hell and I. Gresits, *Org. Biomol. Chem.*, 2010, **8**, 4575–4581.
26 M. Kidwai, V. Bansal, A. Kumar and S. Mozumdar, *Green Chem.*, 2007, **9**, 742–745.
27 A. S.-Y. Lee, G.-A. Chen, Y.-T. Chang and S.-F. Chu, *Synlett*, 2009, 441–446.
28 V. K. Y. Lo, Y. G. Liu, M. K. Wong and C. M. Che, *Org. Lett.*, 2006, **8**, 1529–1532.
29 J. V. Madhav, B. S. Kuarm, P. Someshwar, B. Rajitha, Y. T. Reddy and P. A. Crooks, *Synth. Commun.*, 2008, **38**, 3215–3223.
30 O. P. Pereshivko, V. A. Peshkov and E. V. Van der Eycken, *Org. Lett.*, 2010, **12**, 2638–2641.
31 C. Wetzel, P. C. Kunz, I. Thiel and B. Spingler, *Inorg. Chem.*, 2011, **50**, 7863–7870.
32 Z. Xu, X. Yu, X. Feng and M. Bao, *J. Org. Chem.*, 2011, **76**, 6901–6905.
33 Q. Zhang, J.-X. Chen, W.-X. Gao, J.-C. Ding and H.-Y. Wu, *Appl. Organomet. Chem.*, 2010, **24**, 809–812.
34 L. Abahmane, J. M. Kohler and G. A. Groß, *Chem.–Eur. J.*, 2011, **17**, 3005–3010.
35 M. L. Kantam, S. Laha, J. Yadav and S. Bhargava, *Tetrahedron Lett.*, 2008, **49**, 3083.
36 G. Villaverde, A. Corma, M. Iglesias and F. Sanchez, *ACS Catal.*, 2012, **2**, 399–406.
37 K. K. R. Datta, B. V. S. Reddy, K. Ariga and A. Vinu, *Angew. Chem., Int. Ed.*, 2010, **49**, 5961–5965.
38 K. Layek, R. Chakravarti, M. L. Kantam, H. Maheswaran and A. Vinu, *Green Chem.*, 2011, **13**, 2878–2887.
39 K. M. Reddy, N. S. Babu, I. Suryanarayana, P. S. Sai Prasad and N. Lingaiah, *Tetrahedron Lett.*, 2006, **47**, 7563–7566.
40 G. Shore, W.-J. Yoo, C.-J. Li and M. G. Organ, *Chem.–Eur. J.*, 2010, **16**, 126–133.
41 L. Liu, X. Zhang, J. Gao and C. Xu, *Green Chem.*, 2012, **14**, 1710–1720.
42 V. A. Peshkov, O. P. Pereshivko and E. V. Van der Eycken, *Chem. Soc. Rev.*, 2012, **41**, 3790–3807.
43 (*a*) J. Schäferhans, S. Gómez-Quero, D. V. Andreeva and G. Rothenberg, *Chem.–Eur. J.*, 2011, **17**, 12254–12256; (*b*) J. Dulle, S. Nemeth, E. V. Skorb, T. Irrgang, J. Senker, R. Kempe, A. Fery and D. V. Andreeva, *Adv. Funct. Mater.*, 2012, **22**, 3128–3135.
44 D. V. Andreeva, *Int. J. Mater. Res.*, 2011, **102**, 597–598.
45 N. Pazos-Perez, T. Borke, D. V. Andreeva and R. A. Alvarez-Puebla, *Nanoscale*, 2011, **3**, 3265–3268.
46 E. V. Skorb, D. Fix, D. G. Shchukin, H. Möhwald, D. V. Sviridov, R. Mousa, N. Wanderka, J. Schäferhans, N. Pazos-Pérez, A. Fery and D. V. Andreeva, *Nanoscale*, 2011, **3**, 985–993.
47 N. Pazos-Pérez, J. Schäferhans, E. V. Skorb, A. Fery and D. V. Andreeva, *Microporous Mesoporous Mater.*, 2011, **154**, 164–169.
48 C.-J. Li and C. Wei, *Chem. Commun.*, 2002, 268.
49 L. T. Shi, Y.-Q. Tu, M. Wang, F.-M. Zhang and C.-A. Fan, *Org. Lett.*, 2004, **6**, 1001.
50 S. H. H. Zaidi, R. Halder, K. S. Singh, J. Das and J. Iqbal, *Tetrahedron Lett.*, 2002, **43**, 6485.
51 G. W. Kabalka, L. Wang and R. M. Pagni, *Synlett*, 2001, 676.
52 M. J. Albaladejo, F. Alonso, Y. Moglie and M. Yus, *Eur. J. Org. Chem.*, 2012, 3093–3104.
53 (*a*) S. Brunauer, L. S. Deming, W. E. Deming and E. Teller, *J. Am. Chem. Soc.*, 1940, **62**, 1723; (*b*) IUPAC Commission on Colloid and Surface Chemistry Including Catalysis, *Pure Appl. Chem*, 1985, **57**, 603–619.
54 S. Velu, K. Suzuki, M. Vijayaraj, S. Barman and C. S. Gopinath, *Appl. Catal., B*, 2005, **55**, 287.
55 M. Vijayaraj and C. S. Gopinath, *J. Catal.*, 2006, **241**, 83.